Screening of pair fluctuations in superconductors with coupled shallow and deep bands: A route to higher-temperature superconductivity

L. Salasnich,[1,2] A. A. Shanenko,[3] A. Vagov,[4,5] J. Albino Aguiar,[3] and A. Perali[6]

[1]*Dipartimento di Fisica e Astronomia "Galileo Galilei," Università di Padova, Via Marzolo 8, 35131 Padova, Italy*

[2]*Istituto Nazionale di Ottica (INO) del Consiglio Nazionale delle Ricerche (CNR), Sezione di Sesto Fiorentino, Via Nello Carrara 2, 50019 Sesto Fiorentino, Italy*

[3]*Departamento de Física, Universidade Federal de Pernambuco, Av. Jorn. Aníbal Fernandes, s/n, Cidade Universitária 50740-560, Recife, PE, Brazil*

[4]*Institut für Theoretische Physik III, Bayreuth Universität, Bayreuth 95440, Germany*

[5]*ITMO University, 49 Kronverksky Pr., St. Petersburg 197101, Russia*

[6]*School of Pharmacy, Physics Unit, Università di Camerino, I-62032-Camerino, Italy*

(Received 8 October 2018; revised manuscript received 4 July 2019; published 12 August 2019)

A combination of strong Cooper pairing and weak superconducting fluctuations is crucial to achieve and stabilize high-T_c superconductivity. We demonstrate that a coexistence of a shallow carrier band with strong pairing and a deep band with weak pairing, together with the Josephson-like pair transfer between the bands to couple the two condensates, realizes an optimal multicomponent superconductivity regime: it preserves strong pairing to generate large gaps and a very high critical temperature but screens the detrimental superconducting fluctuations, thereby suppressing the pseudogap state. Surprisingly, we find that the screening is very efficient even when the interband coupling is very small. Thus, a multiband superconductor with a coherent mixture of condensates in the BCS regime (deep band) and in the BCS-BEC crossover regime (shallow band) offers a promising route to higher critical temperatures.

DOI: 10.1103/PhysRevB.100.064510

I. INTRODUCTION

Multiband and multigap superconductors have demonstrated a potential to exhibit novel coherent quantum phenomena that can enhance the pairing energy and the critical temperature T_c [1]. The well-known examples are magnesium diboride [2–4] and iron-based superconductors [5,6], where multiple Fermi surfaces can be effectively controlled by doping or by applying pressure [7,8]. Multiband superconductivity can also be achieved in artificial inhomogeneous structures made of a single-band superconducting material—nanofilms, nanostripes, or samples with spatially controlled impurity distributions [9–12].

The phenomenon entangled with the multiband superconductivity, important in this work, is the BCS-BEC crossover [13–16]. Proximity to this crossover in multiband materials with deep and shallow bands can give rise to a notable increase of superconducting gaps [17–20], which on the mean-field level leads to higher T_c. The physical reason is the depletion of the Fermi motion in a shallow band, which yields short-sized pairs. In such materials, the superconducting state is a coherent mixture of a BCS condensate in deep bands and the BCS-BEC crossover or even nearly BEC condensate in shallow bands. This takes place in, e.g., MgB_2 [19], many iron-based superconductors [8,21–24], and in nanoscale samples [17,18]. Besides the widely explored case of the BCS-BEC crossover in the FeSe family of superconductors, interestingly enough in the Co-doped $LiFe_{1-x}Co_xAs$, with a critical temperature in the range 15–18 K, the BEC regime has been detected for increasing Co doping, with a large superconducting gap opening even when the chemical potential is below one of the conduction bands [25].

However, the largest enemy of the high-T_c superconductivity in such materials is superconducting fluctuations. They are significant for the same reason, which leads to a higher T_c—the depletion of the carrier motion in a shallow band that is associated with a low superconducting stiffness. The fluctuations give rise to the pseudogap state in the interval $T_c < T < T_{c0}$, where T_{c0} extracted from the mean-field calculations marks the appearance of incoherent and short-lived Cooper pairs. The latter develop a coherent state below T_c—the true critical temperature of the superconducting condensate [26,27]. For shallow bands, $T_c \ll T_{c0}$ and this eliminates all gains of the BCS-BEC crossover regime.

In this paper, we consider the mechanism to suppress these fluctuations, which involves the interference of multiple pairing channels with significantly different stiffness. In particular, we investigate how the fluctuation-induced shift in the critical temperature of a superconductor with one shallow and one deep band is affected by the Josephson-like pair transfer between the bands. Our results demonstrate that even a very small coupling to the stable condensate of a deep band is enough to screen severe superconducting fluctuations and "kill" the pseudogap regime, thereby stabilizing the BCS-BEC-crossover condensate of the shallow band at high temperatures. While a similar effect has been included previously to model the momentum-dependent interactions in underdoped cuprates [28] and to study the vortex states [29], only in the present paper is fluctuation screening proposed as a key mechanism for stabilizing a higher T_c.

II. GINZBURG-LANDAU FUNCTIONAL

We adopt the standard microscopic model of a two-band superconductor introduced in [30,31], with deep ($\nu = 1$) and shallow ($\nu = 2$) bands. The conventional s-wave pairing is assumed for both bands, with the symmetric real coupling matrix $\check{g}$ and its elements $g_{\nu\nu'}$. The intraband coupling $g_{\nu\nu}$ is chosen so that the shallow-band mean-field critical temperature is significantly larger than the deep-band one for the zero Josephson-like coupling $g_{12} = 0$. The parabolic dispersion is adopted for both bands $\varepsilon_{\nu,k} = \varepsilon_{\nu,0} + \hbar^2 k^2/2m_\nu$, with $\varepsilon_{\nu,0}$ the lowest energy of the band and m_ν the band effective mass. For the deep band $\mu \gg \varepsilon_{1,0}$ (μ is the chemical potential), whereas for the shallow one $\mu \approx \varepsilon_{2,0}$; below we set $\mu = \varepsilon_{2,0}$ for simplicity. For illustration we choose two-dimensional (2D) bands (many multiband materials exhibit quasi-2D Fermi surfaces). The system is assumed in the clean limit.

The fluctuations are calculated using the two-band free-energy functional that in the Ginzburg-Landau (GL) domain is written as [32–39]

$$F = \int d^2\mathbf{r}\left[\sum_{\nu=1}^{2} f_\nu + (\vec{\Delta}, \check{L}\vec{\Delta})\right],$$
$$f_\nu = a_\nu|\Delta_\nu|^2 + \frac{b_\nu}{2}|\Delta_\nu|^4 + \mathcal{K}_\nu|\nabla\Delta_\nu|^2,$$
$$\check{L} = \check{g}^{-1} - \begin{pmatrix} \mathcal{A}_1 & 0 \\ 0 & \mathcal{A}_2 \end{pmatrix}, \tag{1}$$

where $\vec{\Delta} = (\Delta_1, \Delta_2)^T$, $(.,.)$ is the scalar product in the band space, and the coefficients read [29]

$$\mathcal{A}_\nu = N_\nu \ln\left(\frac{2e^\gamma \hbar\omega_c}{\pi T_{c0}}\right), \quad a_\nu = \alpha_\nu(T - T_{c0}),\ \alpha_\nu = \frac{N_\nu}{T_{c0}},$$
$$b_\nu = \frac{7\zeta(3)}{8\pi^2}\frac{N_\nu}{T_{c0}^2},\ \mathcal{K}_\nu = \mathcal{M}_{\mathcal{K},\nu}\frac{N_\nu\hbar^2 v_\nu^2}{T_{c0}^2}, \tag{2}$$

where N_ν is the band density of states, T_{c0} is the mean-field critical temperature of the two-band system, $\hbar\omega_c$ denotes the energy cutoff (the same for both bands), γ is the Euler constant, $\zeta(x)$ is the Riemann zeta function, $\mathcal{M}_{\mathcal{K},1} = \frac{7\zeta(3)}{32\pi^2}$, $\mathcal{M}_{\mathcal{K},2} = \frac{3\zeta(2)}{8\pi^2}$, and the characteristic band velocities are $v_1 = \sqrt{2(\mu - \varepsilon_{1,0})/m_1}$ and $v_2 = \sqrt{2T_{c0}/m_2}$.

T_{c0} is obtained from the linearized gap equation $\check{L}\vec{\Delta} = 0$ [38,39], solved by $\vec{\Delta} = \psi\vec{\eta}$, where ψ is the order parameter and $\vec{\eta}$ is an eigenvector of $\check{L}$ with the zero eigenvalue (see also Appendix A). Then T_{c0} is the largest of the two solutions of $\det\check{L} = 0$. The eigenvector $\vec{\eta}$ can be represented as $\vec{\eta} = (S^{-1/2}, S^{1/2})^T$ with [38]

$$S = \frac{1}{2\lambda_{12}}\left[\lambda_{22} - \frac{\lambda_{11}}{\chi} + \sqrt{\left(\lambda_{22} - \frac{\lambda_{11}}{\chi}\right)^2 + 4\frac{\lambda_{12}^2}{\chi}}\right], \tag{3}$$

where $\chi = N_2/N_1$ and $\lambda_{\nu\nu'} = g_{\nu\nu'}(N_1 + N_2)$. For the critical temperature one obtains

$$T_{c0} = \frac{2e^\gamma}{\pi}\hbar\omega_c \exp\left[-\frac{(1+\chi)(\lambda_{22} - \lambda_{12}S)}{\lambda_{11}\lambda_{22} - \lambda_{12}^2}\right]. \tag{4}$$

Next we rewrite Eq. (1) using the substitution $\vec{\Delta} = \psi\vec{\eta} + \phi\vec{\xi}$, where $\vec{\xi}$ is orthogonal to $\vec{\eta}$. One finds

$$F = \int d^2\mathbf{r}(f_\psi + f_\phi + f_{\psi\phi}), \tag{5}$$

where

$$f_\psi = a_\psi|\psi|^2 + \frac{b_\psi}{2}|\psi|^4 + \mathcal{K}_\psi|\nabla\psi|^2, \tag{6}$$

while f_ϕ is obtained from Eq. (6) by changing $\phi \to \psi$ (also in a_ψ, b_ψ, and $\mathcal{K}_\psi$), and $f_{\psi\phi}$ comprises coupling terms between the modes ψ and ϕ. One notes that only f_ψ describes the critical behavior of the system while f_ϕ adds small noncritical corrections. This difference follows from the fact that $a_\psi = 0$ at $T = T_{c0}$, whereas $a_\phi = (\vec{\xi}, \check{L}\vec{\xi}) \neq 0$ in the same limit (see also Appendix A). Consequently, in the GL domain both the mean-field solution [38] and the fluctuations are defined by the single-component GL functional f_ψ of Eq. (6). The related coefficients read

$$\alpha_\psi = \frac{\alpha_1}{S} + \alpha_2 S, \quad b_\psi = \frac{b_1}{S^2} + b_2 S^2, \quad \mathcal{K}_\psi = \frac{\mathcal{K}_1}{S} + \mathcal{K}_2 S, \tag{7}$$

and $a_\psi = \alpha_\psi(T - T_{c0})$.

III. FLUCTUATION-DRIVEN SHIFT OF T_{c0}

In weakly coupled superconductors, T_{c0} is the superconducting transition temperature at which Cooper pairs are created and form the condensate state. However, in the vicinity of the BCS-BEC crossover the fluctuations destroy the condensate near T_{c0} so that the superconducting transition takes place at $T_c < T_{c0}$. In the interval $T_c < T < T_{c0}$ the system is in the pseudogap regime of incoherent and fluctuating Cooper pairs [15,16,26,27].

The actual transition temperature T_c is obtained by calculating the fluctuation corrections to the mean-field result T_{c0}. Since the fluctuations are determined by the single-component GL functional, the calculation can be done using standard approaches, e.g., the diagrammatic method [40], the renormalization group (RG) [41], or the perturbative calculation of the superfluid density [40]. Here, for the sake of simplicity, we obtain T_c by a method based on the mean-field treatment of the fluctuation-mode interactions.

We split the order parameter into "slow" (fluctuation averaged part) $\varphi(\mathbf{r})$ and "fast" (fluctuation) contribution $\eta(\mathbf{r})$ as $\psi(\mathbf{r}) = \varphi(\mathbf{r}) + \eta(\mathbf{r})$. Then, the fluctuation part of Eq. (6) is approximated by the Gaussian "Hamiltonian" that is generally written in the form (for details, see Appendix B)

$$H = \sum_{\mathbf{q}}\left[A_{\mathbf{q}}\left(x_{\mathbf{q}}^2 + y_{\mathbf{q}}^2\right) + B_{\mathbf{q}}(x_{\mathbf{q}}x_{-\mathbf{q}} - y_{\mathbf{q}}y_{-\mathbf{q}})\right], \tag{8}$$

where $\eta_{\mathbf{q}} = x_{\mathbf{q}} + iy_{\mathbf{q}}$, with $\eta_{\mathbf{q}}$ the Fourier transform of $\eta(\mathbf{r})$, and the coefficients for the diagonal and off-diagonal terms $A_{\mathbf{q}}$ and $B_{\mathbf{q}}$ depend on a chosen model for the fluctuations.

The interaction of the fluctuation modes is taken into account in a way similar to the Popov approximation for the fluctuation corrections to the Gross-Pitaevskii equation [42,43]. In this way, in addition to the linear terms, higher powers of η are

retained in the GL equation and then linearized within a mean-field approximation. The corresponding fluctuation-averaged GL equation is given by (the subscript ψ of the coefficients a, b, and $\mathcal{K}$ is suppressed below)

$$(a + 2b\langle|\eta|^2\rangle)\varphi + b\varphi|\varphi|^2 - \mathcal{K}\nabla^2\varphi = 0, \tag{9}$$

where $\langle\cdots\rangle$ stands for the fluctuation averaging. For "Hamiltonian" (8) one obtains $\langle\eta\rangle = \langle\eta|\eta|^2\rangle = \langle\nabla^2\eta\rangle = 0$. The anomalous average $\langle\eta^2\rangle$ is zero only when $B_{\mathbf{q}} = 0$. However, in practical cases $|A_{\mathbf{q}}| \gg |B_{\mathbf{q}}|$ [40], which means that $|\langle\eta^2\rangle| \ll \langle|\eta|^2\rangle$, and $\langle\eta^2\rangle$ can be ignored (this is equivalent to the random phase approximation). In our calculation, $B_{\mathbf{q}} = 0$ [see Eq. (10) below].

At $T \geqslant T_c$ we have $\varphi = 0$, and hence η obeys the standard GL equation resulting from (6). This equation is linearized by invoking the mean-field approximation $\eta|\eta|^2 \approx 2\eta\langle|\eta|^2\rangle$, where the factor 2 ensures the critical enhancement of fluctuations at $T = T_c$. This yields

$$A_{\mathbf{q}} = a + 2b\langle|\eta|^2\rangle + \mathcal{K}q^2, \quad \langle|\eta|^2\rangle = \frac{1}{L^2}\sum_{\mathbf{q}}\frac{T}{A_{\mathbf{q}}}, \tag{10}$$

while $B_{\mathbf{q}} = 0$.

The shifted transition temperature is obtained from the condition that the linear term in Eq. (9) vanishes, yielding

$$T_c = T_{c0} - \frac{2b\langle|\eta|^2\rangle_c}{\alpha}, \tag{11}$$

where $\langle|\eta|^2\rangle_c$ is calculated at $T = T_c$ and given by a formally divergent integral

$$\langle|\eta|^2\rangle_c = \int\limits_{\Lambda_0<q<\Lambda_\infty} \frac{d^2\mathbf{q}}{(2\pi)^2}\,\frac{T_c}{\mathcal{K}q^2} = \frac{T_c}{2\pi\mathcal{K}}\ln\left(\frac{\Lambda_\infty}{\Lambda_0}\right), \tag{12}$$

regularized by the infrared Λ_0 and ultraviolet Λ_∞ cutoffs. The latter is determined by the applicability of the GL theory, which limits the spatial fluctuation length by the BCS coherence length $\xi(0)$ so that $\Lambda_\infty = 1/\xi(0)$ [40]. The upper limit of the fluctuation field length is naturally related to the GL coherence length $\xi(T_{\mathrm{Gi}})$, calculated at the Ginzburg-Levanyuk temperature $T_{\mathrm{Gi}} = T_{c0}(1 - \mathrm{Gi})$. Recall that Gi defines the interval in the vicinity of T_{c0}, where the mean-field theory is compromised by fluctuations and for the case of interest $\mathrm{Gi} = b/(4\pi\alpha\mathcal{K})$. The renormalization-group (RG) analysis yields $\Lambda_0 = 2/\xi(T_{\mathrm{Gi}})$; see Appendix C for details. Using the standard definition of the GL coherence length $\xi = \sqrt{-\mathcal{K}/a}$, one obtains

$$\frac{\delta T_c}{T_c} \equiv \frac{T_{c0} - T_c}{T_c} = 2\,\mathrm{Gi}\,\ln\left(\frac{1}{4\,\mathrm{Gi}}\right), \tag{13}$$

which recovers the known two-dimensional RG result for the critical temperature shift at $\mathrm{Gi} \to 0$ [40]. The corresponding RG analysis is outlined in Appendix C, where we demonstrate that the RG shift of the mean-field critical temperature is the same as that obtained in the main paper in the range of validity of our approximations, supporting the robustness of our results, even when a more refined theoretical approach is applied.

We note in passing that when the system enters the Berezinskii-Kosterlitz-Thouless (BKT) regime with large fluctuations, the temperature shift can be estimated using the Nelson-Kosterlitz criterion [44], which yields $(\delta T_c/T_c)_{\mathrm{BKT}} \propto \mathrm{Gi}$ (see Fig. 15.1 of [40] and Appendix D). However, as we demonstrate, here the fluctuations are suppressed by the coupling to the deep band, and therefore the critical temperature shift is determined by Eq. (13).

IV. RESULTS

To investigate the sensitivity of the pair fluctuations to the interband coupling, we consider the limit $v_2/v_1 \to 0$ (as $v_2 \ll v_1$) so that $\mathrm{Gi} = b/(4\pi\alpha\mathcal{K})$ [b, α, and $\mathcal{K}$ are given by Eq. (7), and the subscript ψ is suppressed] is reduced to

$$\mathrm{Gi} = \mathrm{Gi}_{\mathrm{deep}}\frac{1 + S^4}{1 + S^2}, \tag{14}$$

with S given by Eq. (3) and $\mathrm{Gi}_{\mathrm{deep}}$ the Ginzburg number of the deep band. (A similar calculation of the effective Gi number has been done in Ref. [29] to study the effect of fluctuations in the intertype domain of a multiband superconductor with magnetic field.) The latter depends on $\mu - \varepsilon_{1,0}$ and is a tuneable parameter assuming small enough values. T_{c0} and T_c as functions of λ_{12} are found from Eqs. (3), (4), (13), and (14), where we use $\lambda_{11} = 0.25$ and $\lambda_{22} = 0.30$, and $N_1 = N_2$. Our qualitative conclusions are not sensitive to a particular choice of λ_{11}, λ_{22}, and $\chi = N_2/N_1$. The only restriction is that the mean-field critical temperature of the uncoupled shallow band $T_{c0,2}$ is significantly larger than that of the deep band $T_{c0,1}$.

Obtained T_{c0} and T_c are shown in units of $T_{c0,1}$ in Fig. 1 ($T_{c0,2}$ is also given as a guide for the eye). Three panels are for $\mathrm{Gi}_{\mathrm{deep}} = 10^{-5}$ (a), 10^{-4} (b), and 10^{-3} (c). The validity range of our results is given by $\mathrm{Gi} \lesssim 1/(4e)$, where $1/(4e) \approx 0.092$ is the maximum of the right-hand side of Eq. (13). At larger Gi, Eq. (13) cannot be applied, which reflects a huge impact of the fluctuations.

Strikingly, the results in Fig. 1 reveal that the fluctuations are screened almost completely even for extremely small values of λ_{12}, especially when the fluctuations of the BCS condensate in the deep band are weak enough. For example, for $\mathrm{Gi}_{\mathrm{deep}} = 10^{-5}$ [Fig. 1(a)] the pseudogap interval becomes negligible at $\lambda_{12} \simeq 0.002 \approx 0.01\lambda_{22}$. Here the system is in the BCS-BEC crossover regime, governed by the shallow band, but T_c is close to $T_{c0,2}$.

Notice that for real materials, λ_{12} is usually in the range $0.005 \lesssim \lambda_{12} \lesssim 0.4$ (see Ref. [45] and references therein). Also, the chosen values of $\mathrm{Gi}_{\mathrm{deep}}$ are in line with conservative estimations for materials with 2D bands [46]. Finally, we recall that although our calculations are performed for $\mu = \varepsilon_{2,0}$ (for simplicity), increasing the Lifshitz parameter $(\mu - \varepsilon_{2,0})/\varepsilon_{2,0}$ does not change our conclusions as long as $v_1 \gg v_2$.

Suppression of fluctuations can be qualitatively explained by noting that the bands contribute differently to the coefficients of the effective single-component GL functional (6), which determines both T_{c0} and fluctuations. Its coefficients are given by Eq. (7) as sums of the band contributions with the weight factors that are powers of S for the shallow band and of S^{-1} for the deep one. In the presence of the strong shallow band, $S \gg 1$, so that coefficients a and b are determined mainly by that band. However, the stiffness $\mathcal{K}$ is controlled

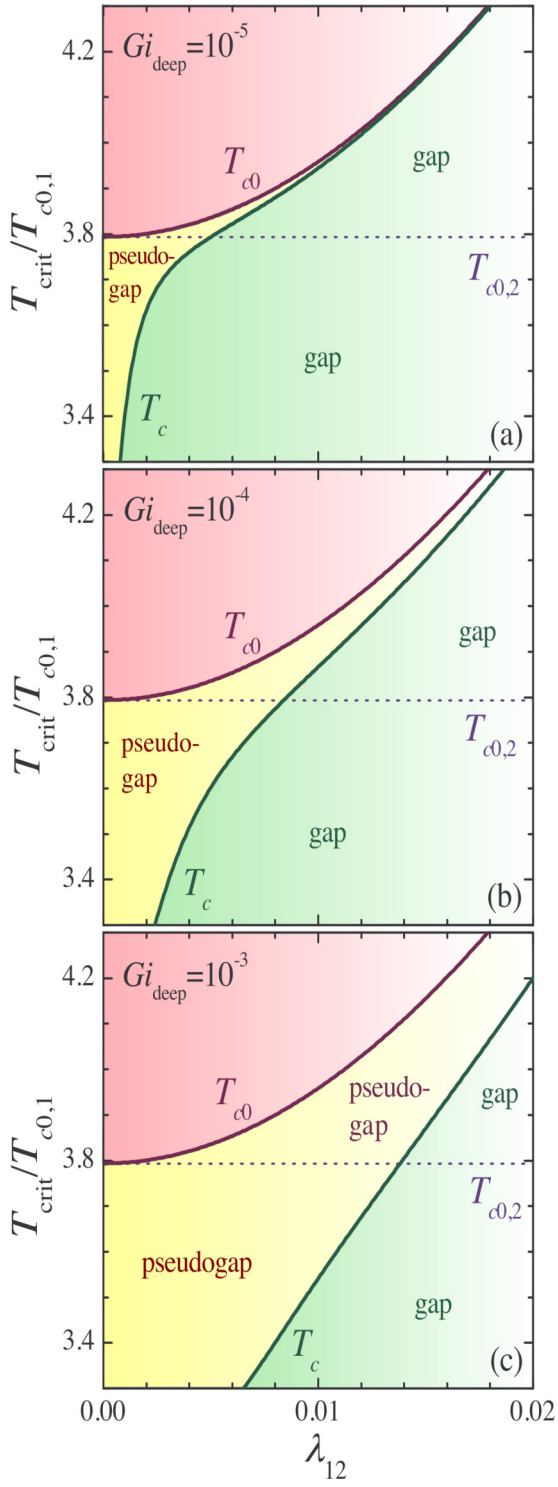

FIG. 1. The mean-field and fluctuation-shifted critical temperatures T_{c0} and T_c vs the interband coupling λ_{12}. Panels (a)–(c) correspond to $\mathrm{Gi}_{\mathrm{deep}} = 10^{-5}$, 10^{-4}, and 10^{-3}, respectively. The mean-field transition temperature of the uncoupled shallow band $T_{c0,2}$ is given as a reference value.

by the deep band, because $\mathcal{K}_2$ is proportional to the square of the nearly zero characteristic carrier velocity in the shallow band. This implies that the "light" condensate excitations in the shallow band are necessarily accompanied ("dressed" or "screened") and suppressed by the "heavy" excitations in the deep band. The only exception is the case of a vanishingly small interband coupling $\lambda_{12} \to 0$ for which $S^{-1} \to 0$ so that the influence of the deep band condensate is "switched off."

V. DISCUSSIONS AND CONCLUSIONS

As previously mentioned, we do not claim that the fluctuation screening mechanism, based on the interference of multiple pairing channels with different stiffness, is the only possible scenario to obtain a higher critical temperature. Clearly, other effects can give rise to a higher critical temperature. However, whatever those mechanisms might be, the respective transition temperature T_c is calculated within the mean-field approach.

For example, it has been recently demonstrated [47] that even within the standard BCS theory, the interplay between the interparticle distance and the finite range of the pairing potential gives rise to a domelike shape of the density dependence of T_c with a clearly defined maximum. This can be used to optimize the system for the highest T_c. This prediction can be further improved by invoking the Eliashberg approach to take into account the dynamics of the pairing and the Coulomb repulsion.

However, neither of those mean-field mechanisms of reaching a higher T_c takes into account the crucial effect of superconducting fluctuations, which grows in importance with the increasing ratio T_c/E_F (E_F is the Fermi energy). Consequently, one must still overcome the problem of large fluctuations that always accompany this high mean-field T_c. Hence, once the mean-field problems toward high T_c are overcome, we remain with the problem of avoiding severe fluctuations you might find in low-dimensional systems, in the moderate and strong-coupling regime of pairing, and in low-density systems. Our work points toward a bright mechanism to solve this ultimate obstacle to reach a very high-temperature superconductivity.

This work focuses on the regime of the weak-to-moderate pairing coupling. This regime is, however, relevant even for the room-temperature superconductivity. As an example, we point to metallo-organic materials (e.g., K-doped paraterphenyl) or the newly discovered class of superhydrides that have dimensionless couplings of the order of $\lambda = 0.3$–0.4 but very large phononic frequencies, exceeding 100 meV (1160 K). These materials have a multiband electronic structure and reveal Lifshitz transitions [20,48,49] and thus are relevant for the analysis of this work. Hence, the coupling of the equation for the critical temperature (given by the Thouless criterion) with the density equation for the chemical potential can be disregarded at this level, being overall the system of our interest at the BCS side of the BCS-BEC crossover.

In the case of two-band or two-component ultracold atomic fermions, in order to investigate the BCS-BEC crossover in the two-band configuration from the weak-interaction (BCS side) to the strong-interaction (BEC side) regimes, the coupling of the equation for the critical temperature with the density equation for the chemical potential is indeed crucial, differently from the case considered in the paper.

In conclusion, this paper reveals a very effective mechanism to suppress the pairing fluctuations in a two-band superconductor with one deep and one shallow band. The shallow band is in the regime of the BCS-BEC crossover, where the mean-field critical temperature is expected to be high. Although superconducting fluctuations in the shallow band alone are very large and would normally destroy the superconductivity, they are screened by the pair transfer to the deep band. Remarkably, the suppression is very effective, almost complete, even when the interband coupling is so small that the superconducting temperature is fully determined by the shallow band. Our results provide a solid explanation of the recent striking observation that the pseudogap was not detected in the multiband BCS-BEC-crossover superconductor FeSe, which was called by the authors "a unique feature that is absent in a single band system". Notice that superconductivity is the most robust phase with respect to other instabilities that can arise when shallow bands and high density of states are present in the system.

This opens new perspectives in searching for novel multiband superconductors with higher critical temperatures as the fluctuation screening arising from the interference of multiple pairing channels is a fundamental mechanism to protect the superconductivity. One notes that many other scenarios have been proposed to achieve a high T_c—an interplay between the finite-range pairing potential and the interparticle distance is one of the latest [47]. However, all those are based on the mean-field analysis and neglect enhanced fluctuations. The present mechanism is a unique one to avoid severe superconducting fluctuations being an ultimate obstacle toward very high superconducting temperatures.

Finally, we point to the universality of this screening mechanism that can also suppress particle-hole fluctuations in multiband charge or spin ordered systems, expanding the applicability of our results. For example, it can be relevant for multiband superfluidity of ultracold fermions in optical lattices [50,51], for multiorbital fermions with pairing of different channels [52], and also for electron-hole superfluids in double-bilayer graphene devices [53] that can have multicomponent effects [54].

ACKNOWLEDGMENTS

The authors acknowledge support from the Brazilian agencies Conselho Nacional de Ciência e Tecnologia, CNPq (Grants No. 307552/2012-8, No. 309374/2016-2, and No. 484504/2013-4) and Funadação de Amparo a Ciência e Tecnologiado Estado de Pernambuco, FACEPE (APQ-0936-1.05/15). A.P. acknowledges the financial support from Universidade Federal de Pernambuco (Grant No. 23076.006072/2015-77) during his visit in 2015, and also the financial support from the Italian MIUR through the PRIN 2015 program, Contract No. 2015C5SEJJ001. A.S. and A.V. acknowledge the hospitality of the Departamento de Física da Universidade Federal de Pernambuco during their temporary stays in the years 2013–2017, and the financial support from CNPq (Grants No. 452740/2013-4 and No. 400510/2014-6) and FACEPE (Grant No. ARC 0249-1/13). L.S. acknowledges partial support from FFABR grant of Italian MIUR. A.V. acknowledges support from the Russian Science Foundation, Project 18-12-00429. The authors thank A. Bianconi, P. Pieri, and A. A. Varlamov for useful discussions and acknowledge the collaboration within the MultiSuper International Network [55].

APPENDIX A: DETAILS OF GINZBURG-LANDAU FUNCTIONAL FOR TWO BANDS

We consider a standard microscopic model of a two-band superconductor as described in Refs. [30,31]. The conventional s-wave pairing in both bands is controlled by the intraband interaction strength $g_{\nu\nu}$ ($\nu = 1, 2$) and the interband coupling $g_{12} = g_{21}$ of the Josephson type. We assume one band is deep ($\nu = 1$) and the other is shallow $\nu = 2$, and both bands are two-dimensional with the parabolic dispersion. We consider a system in the clean limit, i.e., without impurity potential. The mean-field Hamiltonian of the model reads

$$\mathcal{H} = \sum_{\nu=1,2} \int d^2\mathbf{r}\, [\hat{\psi}^\dagger_{\nu\sigma}(\mathbf{r})\, T_\nu(\mathbf{r})\, \hat{\psi}_{\nu\sigma}(\mathbf{r}) + [\hat{\psi}^\dagger_{\nu\uparrow}(\mathbf{r})\hat{\psi}^\dagger_{\nu\downarrow}(\mathbf{r})\, \Delta_\nu(\mathbf{r}) + \text{H.c.}]] + (\vec{\Delta}, \check{g}^{-1}\vec{\Delta}), \quad \text{(A1)}$$

where $\hat{\psi}^\dagger_{\nu\sigma}(\mathbf{r})$ and $\hat{\psi}_{\nu\sigma}(\mathbf{r})$ are the field operators for the charge carriers in band ν ($\nu = 1, 2$), and $T_\nu(\mathbf{x})$ is the single-particle energy minus the chemical potential. We use the vector notation $\vec{\Delta} = (\Delta_1, \Delta_2)^T$ with band gaps $\Delta_{\nu=1,2}$ and the scalar product defined as $(\vec{A}, \vec{B}) = \sum_\nu A^*_\nu B_\nu$. Finally, $\check{g}^{-1}$ is the inverse of the coupling matrix $\check{g}$ with elements $g_{\nu\nu'}$.

The Hamiltonian $\mathcal{H}$ is to be solved with the self-consistency condition

$$\vec{\Delta} = \check{g}\vec{R}, \quad \text{(A2)}$$

where $\vec{R} = (R_1, R_2)^T$ and $R_\nu = \langle\hat{\psi}_{\nu\uparrow}(\mathbf{r})\hat{\psi}_{\nu\downarrow}(\mathbf{r})\rangle$, with $\langle\cdots\rangle$ denoting the statistical average. Near the mean-field critical temperature T_{c0} the anomalous Green function R_ν can be approximated as (see, e.g., [38,39])

$$R_\nu[\Delta_\nu] \simeq \mathcal{A}_\nu\Delta_\nu + \Omega_\nu[\Delta_\nu], \quad \text{(A3)}$$

with

$$\Omega_\nu[\Delta_\nu] = -a_\nu\Delta_\nu - b_\nu\Delta_\nu|\Delta_\nu|^2 + \mathcal{K}_\nu\nabla^2\Delta_\nu, \quad \text{(A4)}$$

where the coefficients $\mathcal{A}_\nu$, a_ν, b_ν, and $\mathcal{K}_\nu$ are given by Eq. (2) in the text. Notice that the zero-field case is considered. Then, the self-consistency condition (A2) is represented as the matrix gap equation

$$\check{L}\vec{\Delta} = \vec{\Omega}, \quad \text{(A5)}$$

where $\vec{\Omega} = (\Omega_1, \Omega_2)^T$ and the matrix $\check{L}$ is defined by Eq. (1) in the paper. The solution to Eq. (A5) is the stationary point of the free-energy functional given by Eq. (1) in the paper.

The mean-field transition temperature T_{c0} is obtained from the linearized matrix gap equation $\check{L}\vec{\Delta} = 0$ [38,39], which can be explicitly written as

$$\begin{pmatrix} g_{22} - G\mathcal{A}_1 & -g_{12} \\ -g_{12} & g_{11} - G\mathcal{A}_2 \end{pmatrix}\begin{pmatrix}\Delta_1 \\ \Delta_2\end{pmatrix} = 0. \quad \text{(A6)}$$

Notice that $a_\nu \to 0$ for $T \to T_{c0}$ [see Eq. (2) of the text] and so the term $a_\nu\Delta_\nu$ does not contribute to Eq. (A6). The solution

to this equation is represented as

$$\vec{\Delta} = \psi(\mathbf{r})\vec{\eta}, \tag{A7}$$

where $\vec{\eta} = (\eta_1, \eta_2)^T$ is an eigenvector of $\check{L}$ corresponding to its zero eigenvalue, and $\psi(\mathbf{r})$ is the Landau order parameter that controls the spatial distribution of both band condensates [38,39]. Notice that the linearized gap equation does not give any information about such a distribution, and one should go beyond the linearized equation to find ψ [38]. The appearance of the single-component order parameter in the equation for the mean-field critical temperature T_{c0} is connected with the mean-field description of a two-band superconductor by the single-component Ginzburg-Landau (GL) formalism [38]. This is in agreement with the Landau theory of phase transitions according to which the number of order-parameter components is determined by the relevant irreducible group representation rather than by the number of the contributing bands; see the discussions in [39].

Introducing the quantity

$$S \equiv (g_{22} - G\mathcal{A}_1)/g_{12}, \tag{A8}$$

the equation $\det \check{L} = 0$, which determines T_{c0} (one chooses the largest T_{c0} of the two solutions), is written as

$$1/S = (g_{11} - G\mathcal{A}_2)/g_{12}. \tag{A9}$$

Then, using Eqs. (A8) and (A9), $\vec{\eta}$ can be chosen in the form

$$\vec{\eta} = \begin{pmatrix} S^{-1/2} \\ S^{1/2} \end{pmatrix}. \tag{A10}$$

We remark that the normalization of the eigenvector (A10) is arbitrary—it is absorbed in the order parameter ψ in Eq. (A7). Using Eq. (2) of the text together with Eqs. (A8) and (A9) here, one finds the explicit expressions for S and T_{c0} given by Eqs. (3) and (4) in the paper.

APPENDIX B: DETAILS OF THE GAUSSIAN APPROXIMATION FOR TWO BANDS

To investigate the superconductive fluctuations in the GL domain, we express superconducting gaps Δ_ν using $\vec{\eta}$ and $\vec{\xi}$, where $\vec{\xi}$ is any vector orthogonal to $\vec{\eta}$ (the normalization is not important), as

$$\vec{\Delta} = \psi\vec{\eta} + \phi\vec{\xi}, \tag{B1}$$

where $\phi = \phi(\mathbf{r})$ is a new spatial mode in addition to $\psi(\mathbf{r})$ introduced in the previous section. Using Eq. (B1), the free-energy functional given by Eq. (1) in the main paper is expressed in terms of ψ and ϕ, see Eqs. (5) and (6) in the paper. The relevant coefficients in Eq. (6) of the main text are given by

$$\begin{aligned} a_\psi &= \sum_\nu a_\nu |\eta_\nu|^2, \quad a_\phi = (\vec{\xi}, \check{L}\vec{\xi}) + \sum_\nu a_\nu |\xi_\nu|^2, \\ \mathcal{K}_\psi &= \sum_\nu \mathcal{K}_\nu |\eta_\nu|^2, \quad \mathcal{K}_\phi = \sum_\nu \mathcal{K}_\nu |\xi_\nu|^2, \\ b_\psi &= \sum_\nu b_\nu |\eta_\nu|^4, \quad b_\phi = \sum_\nu b_\nu |\xi_\nu|^4, \end{aligned} \tag{B2}$$

where η_ν and ξ_ν denote components of $\vec{\eta}$ and $\vec{\xi}$. The key difference between the modes ψ and ϕ is that the expression for a_ϕ contains $(\vec{\xi}, \check{L}\vec{\xi})$, which is nonzero because eigenstates of $\check{L}$ are not degenerate. [The eigenvectors corresponding to the zero eigenvalue form a one-dimensional subspace, except for the unrealistic case of two equivalent bands with zero interband coupling.] Taking into account that $a_\nu \to 0$ at $T \to T_{c0}$, one sees that $a_\psi \to 0$ but $a_\phi \not\to 0$ in this limit. This means that the coherence length associated with the mode ϕ is not divergent at T_{c0} (and neither is the corresponding contribution to the heat capacity), while the mode ψ is critical and the corresponding length diverges. Thus, investigating the contribution of the superconducting fluctuations near T_{c0}, one needs to consider only the critical mode ψ. The mode ϕ can be safely neglected and one arrives at the single-component GL description of the superconducting transition with the single-component order parameter ψ; see the discussion in the previous section after Eq. (A7). Using Eq. (A10), one can easily get Eq. (7) of the main text.

To get the Gaussian fluctuation functional, one represents the order parameter ψ as the sum of its "slow" part $\varphi(\mathbf{r})$ (averaged over fluctuations) and "fast" contribution $\eta(\mathbf{r})$ (fluctuations). The standard Gaussian terms in the functional correspond to $|\eta|^2$, η^2, η^{*2}, and $|\nabla\eta|^2$. Then, introducing the real $x_\mathbf{q}$ and imaginary $y_\mathbf{q}$ parts of the Fourier transform of the fluctuation field $\eta_\mathbf{q}$ ($\eta_\mathbf{q} = x_\mathbf{q} + iy_\mathbf{q}$), the fluctuation "Hamiltonian" can generally be written as Eq. (8) in the main paper. The terms involving $x_\mathbf{q}^2$ and $y_\mathbf{q}^2$ come from $|\eta|^2$ and $|\nabla\eta|^2$ whereas $x_\mathbf{q}x_{-\mathbf{q}}$ and $y_\mathbf{q}y_{-\mathbf{q}}$ result from both η^2 and η^{*2}. Performing the standard calculations with the partition function based on Eq. (8), one finds the fluctuation contribution to the free energy in the form

$$F_{\rm fluct} = -\frac{T}{2}\sum_\mathbf{q}\left[\ln\frac{\pi T}{A_\mathbf{q} + B_\mathbf{q}} + \ln\frac{\pi T}{A_\mathbf{q} - B_\mathbf{q}}\right], \tag{B3}$$

which agrees with the expression in the textbook by Larkin and Varlamov [40]. In Eq. (B3), $A_\mathbf{q}$ is the momentum-dependent coefficient for the diagonal term $x_\mathbf{q}^2 + y_\mathbf{q}^2$ in the Gaussian functional, whereas $B_\mathbf{q}$ is the coefficient for the off-diagonal contribution $x_\mathbf{q}x_{-\mathbf{q}} - y_\mathbf{q}y_{-\mathbf{q}}$; see Eq. (8) in the paper.

To find the explicit expressions for $A_\mathbf{q}$ and $B_\mathbf{q}$, one inserts the relation $\psi(\mathbf{r}) = \varphi(\mathbf{r}) + \eta(\mathbf{r})$ into the GL equation for $\psi(\mathbf{r})$ and then averages the resulting expression over the fluctuations. As explained in the paper, when taking into account interactions between the fluctuation fields, the averaging procedure results in Eq. (10) of the text. Subtracting this equation from the initial GL equation for ψ, one finds a rather complicated equation for the fluctuation field η. However, it is significantly simplified for $T \geqslant T_c$, where T_c is the fluctuation-shifted critical temperature. In this case, one finds $A_\mathbf{q}$ and $B_\mathbf{q}$ as given by Eq. (10) of the text.

APPENDIX C: RENORMALIZATION-GROUP ANALYSIS

Equation (13) of the main text can be obtained more rigorously by taking into account the fluctuation corrections using the diagrammatic analysis [40] or, equivalently, by the renormalization group (RG) approach [41]. For the reader's

convenience, we briefly describe how the latter recovers Eq. (13) of the main text. The analysis of the fluctuation effects starts with writing the partition function of the D-dimensional system in the form of the functional integral

$$Z = \int \mathcal{D}[\psi]\ \exp\left(-\frac{1}{T}\int d^D\mathbf{r}\, f(\mathbf{r})\right),$$

$$f(\mathbf{r}) = a|\psi(\mathbf{r})|^2 + \frac{b}{2}|\psi(\mathbf{r})|^4 + \mathcal{K}|\nabla\psi(\mathbf{r})|^2, \tag{C1}$$

with $a = \alpha(T - T_{c0})$, and α, b, and T_{c0} defined in the main text; see Eq. (7) [the index ψ is suppressed]. The fluctuations are studied using the following recursive scheme. First, one splits the functional integral into two parts: the contribution of the "slow" Fourier components $\psi_{\mathbf{q}}$ of $\psi(\mathbf{r})$ with $q < \Lambda$ and the contribution of the "fast" Fourier components with $\Lambda > q$ [42]. If the cutoff Λ is large enough, the contribution of the fast components is small and can be approximated by the Gaussian functional, obtained perturbatively from Eq. (C1). Integrating with respect to the "fast" components changes the remaining "slow"-variables functional. The latter is approximated by the GL form (higher-order contributions are neglected) with the modified coefficients a_Λ and b_Λ ($\mathcal{K}$ is not altered). Then, by introducing the new cutoff $\Lambda' < \Lambda$, the variables in the new functional can also be divided into the "slow" and "fast" ones with $q < \Lambda'$ and $\Lambda' < q < \Lambda$, respectively. Similarly, the integration with respect to these "fast" variables yields another modified GL-like functional of the new "slow" variables with the coefficients $a_{\Lambda'}$ and $b_{\Lambda'}$ given by recursive relations. Considering the cutoff Λ as a continuous variable, one can write these recursive relations for $a_\Lambda(T)$ and $b_\Lambda(T)$ as the following differential equations [40]:

$$\frac{da_\Lambda}{d\Lambda} = -\frac{2T\mu_D b_\Lambda \Lambda^{D-1}}{a_\Lambda + \mathcal{K}\Lambda^2}, \quad \frac{db_\Lambda}{d\Lambda} = \frac{5T\mu_D b_\Lambda^2 \Lambda^{D-1}}{(a_\Lambda + \mathcal{K}\Lambda^2)^2}, \tag{C2}$$

where μ_D depends on the dimensionality D as

$$\mu_D = \frac{D}{2^D \pi^{D/2}\Gamma\left(1+\frac{D}{2}\right)}, \tag{C3}$$

with $\Gamma(\cdot)$ the Euler gamma function.

The connection to the superconductivity transition follows the standard assumption of the RG theory that

$$a_{\Lambda=0}(T_c) = 0 \tag{C4}$$

defines the renormalized (shifted) critical temperature T_c. The theory has the ultraviolet cutoff $\Lambda_\infty = 1/\xi(0)$, with $\xi(0)$ the Cooper pair size [40], at which a_Λ and b_Λ assume their "bare" values given by the standard GL theory $a_{\Lambda=\Lambda_\infty} = a$ and $b_{\Lambda=\Lambda_\infty} = b$; see Eq. (C1).

To solve Eqs. (C2), it is convenient to introduce the scaled variables

$$t = \sqrt{\frac{\mathcal{K}}{\chi}}\Lambda, \quad a_t = \frac{a_\Lambda}{\chi}, \quad b_t = \frac{b_\Lambda}{b}, \tag{C5}$$

with

$$\chi = \mathcal{K}^{-D/(4-D)}(2T\mu_D b)^{2/(4-D)}, \tag{C6}$$

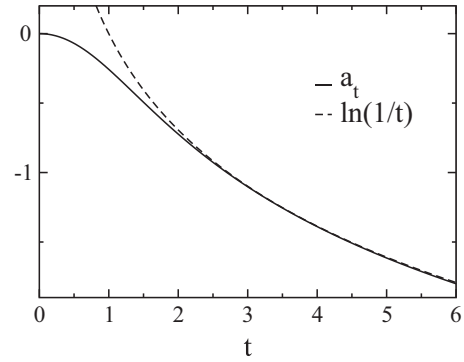

FIG. 2. The solution for a_t (solid line) is plotted together with its large-t asymptote $\ln(1/t)$ (dashed-dotted line).

for which Eqs. (C2) appear in the dimensionless form

$$\frac{da_t}{dt} = -\frac{b_t t^{D-1}}{a_t + t^2}, \quad \frac{db_t}{dt} = \frac{5}{2}\frac{b_t^2 t^{D-1}}{(a_t + t^2)^2}. \tag{C7}$$

These equations are to be solved with the boundary conditions $a_{t=0} = 0$ and $b_{t=t_\infty} = 1$ (with $t_\infty = \sqrt{\mathcal{K}/\chi}\Lambda_\infty$).

Solutions to Eqs. (C7) [and, hence, to Eqs. (C2)] differ qualitatively for different dimensionalities. For the case $D = 3$, one can assume that in the interval of interest $a_t \ll t^2$ and that $b_t \simeq 1$ remains constant, which yields the solution $a_t \simeq t$. Returning to the original variables and inserting the obtained solution in Eq. (C4), one obtains the known result $T_{c0} - T_c \propto T_{c0}\sqrt{\mathrm{Gi}_3}$, with Gi_3 being the Ginzburg number for $D = 3$ [40].

However, for the case $D = 2$ this approximation yields the logarithmic solution that is singular in the lower limit $t \to 0$. Assuming that the solution is restricted by the infrared cutoff t_0 in the lower limit, one obtains

$$a_{t=t_\infty} = a_{t=t_0} - \ln(t_\infty/t_0). \tag{C8}$$

Then applying Eq. (C4) at the lower cutoff expressed in the original units as $\Lambda_0 = t_0\sqrt{Tb/\pi}/\mathcal{K}$, one obtains

$$T_{c0} - T_c = \frac{4\pi b T_c}{\alpha\mathcal{K}} \ln\left(\frac{\Lambda_\infty}{\Lambda_0}\right), \tag{C9}$$

which recovers Eqs. (11) and (12) for the shifted critical temperature in the main text, having the same uncertainty for Λ_0.

It can be shown, however, that the logarithmic singularity for $t \to 0$ in Eq. (C8) is an artefact of the used approximations. It disappears when Eqs. (C7) are solved simultaneously. Indeed, for the complete system one obtains the infrared asymptote $a_t \propto t^2$ ($t \to 0$), as is seen from the numerical solution shown in Fig. 2. However, at $t \gtrsim 2$ the solution a_t can be accurately approximated by its ultraviolet logarithmic asymptote also shown in Fig. 2. Taking this logarithmic approximation for the solution and returning back to the original variables, one recovers Eq. (C9) with the same effective infrared cutoff,

$$\Lambda_0 = \frac{1}{\mathcal{K}}\sqrt{\frac{T_c b}{\pi}} \simeq \frac{1}{\mathcal{K}}\sqrt{\frac{T_{c0} b}{\pi}} = \frac{2}{\xi(\mathrm{Gi})}, \tag{C10}$$

as is used in the main text. Notice that the logarithmic approximation is correct when $t_\infty \gg 2$, which yields the applicability

domain of our results as $\mathrm{Gi} \ll 1/2$. This condition is certainly fulfilled for the typical values of $\mathrm{Gi} = 10^{-3,-4,-5}$ assumed for this work.

APPENDIX D: BKT EFFECTS

To estimate the shift of the critical temperature in the regime of the Berezinskii-Kosterlitz-Thouless (BKT) fluctuations, we take the order parameter $\psi(\mathbf{r})$ in the form

$$\psi(\mathbf{r}) = \psi_0\, e^{i\theta(\mathbf{r})}, \tag{D1}$$

where ψ_0 is the uniform solution of the single-component GL equation given by the functional (6) (the subscript ψ is suppressed) in the main text. As we consider only the phase fluctuations governed by the Nambu-Goldstone field $\theta(\mathbf{r})$, the corresponding free-energy functional is reduced to

$$F = F_0 + \int d^2\mathbf{r}\, \frac{J|\nabla\theta(\mathbf{r})|^2}{2}, \tag{D2}$$

where F_0 results from the uniform solution ψ_0, and $J(T) = 2\mathcal{K}\alpha(T - T_{c0})/b$ is the phase stiffness. The compactness of the phase $\theta(\mathbf{r})$ implies that

$$\oint_{\mathcal{C}} \nabla\theta(\mathbf{r}) \cdot d\mathbf{r} = 2\pi q \tag{D3}$$

for any closed contour $\mathcal{C}$. Here $q = 0, \pm 1, \pm 2, \ldots$ is the integer number associated with the corresponding quantum vortex (positive q) or antivortex (negative q). As shown by Kosterlitz and Thouless [56], in the two-dimensional case ($D = 2$), the total number of quantized vortices varies as a function of the temperature: at zero temperature there are no vortices; however, as the temperature increases, vortices start to appear as the vortex-antivortex pairs. The pairs are bound at low temperatures until the Berezinskii-Kosterlitz-Thouless unbinding transition occurs at $T = T_{\mathrm{BKT}}$. Above T_{BKT} a proliferation of free vortices and antivortices takes place and the global coherence is destroyed. The BKT temperature T_{BKT} for two-dimensional superconductors can be estimated using the expression [56]

$$T_{\mathrm{BKT}} = \frac{\pi}{2} J(T_{\mathrm{BKT}}). \tag{D4}$$

From Eq. (D4) we find

$$\frac{T_c - T_{\mathrm{BKT}}}{T_{\mathrm{BKT}}} = 4\,\mathrm{Gi}, \tag{D5}$$

where $\mathrm{Gi} = b/(4\pi\alpha\mathcal{K})$ is the corresponding Ginzburg number associated with the initial GL functional given by Eq. (6). For large fluctuations, the critical temperature shift is controlled by Eq. (D5). However, one should use Eq. (13) of the main text for the values of the interband coupling at which the pseudogap is washed out, i.e., in the limit $\mathrm{Gi} \to 0$.

[1] M. V. Milošević and A. Perali, Supercond. Sci. Technol. **28**, 060201 (2015).
[2] J. Nagamatsu, N. Nakagawa, T. Muranaka, Y. Zenitani, and J. Akimitsu, Nature (London) **410**, 63 (2001).
[3] D. C. Larbalestier, L. D. Cooley, M. O. Rikel, A. A. Polyanskii, J. Jiang, S. Patnaik, X. Y. Cai, D. M. Feldmann, A. Gurevich, A. A. Squitieri, M. T. Naus, C. B. Eom, E. E. Hellstrom, R. J. Cava, K. F. Regan, N. Rogado, M. A. Hayward, T. He, J. S. Slusky, P. Khalifah, K. Inumaru, and M. Haas, Nature (London) **410**, 186 (2001).
[4] P. C. Canfield and G. W. Crabtree, Phys. Today **56**(3), 34 (2003).
[5] Y. Kamihara, H. Hiramatsu, M. Hirano, R. Kawamura, H. Yanagi, T. Kamiya, and H. Hosono, J. Am. Chem. Soc. **128**, 10012 (2006).
[6] J. Paglione and R. L. Greene, Nat. Phys. **6**, 645 (2010).
[7] A. Bianconi, Nat. Phys. **9**, 536 (2013).
[8] K. Okazaki, Y. Ito, Y. Ota, Y. Kotani, T. Shimojima, T. Kiss, S. Watanabe, C.-T. Chen, S. Niitaka, T. Hanaguri, H. Takagi, A. Chainani, and S. Shin, Sci. Rep. **4**, 4109 (2014).
[9] A. Perali, A. Bianconi, A. Lanzara, and N. L. Saini, Solid State Commun. **100**, 181 (1996).
[10] A. Bianconi, A. Valletta, A. Perali, and N. L. Saini, Physica C **296**, 269 (1998).
[11] A. A. Shanenko, M. D. Croitoru, and F. M. Peeters, Phys. Rev. B **78**, 024505 (2008).
[12] N. Pinto, S. J. Rezvani, A. Perali, L. Flammia, M. V. Milošević, M. Fretto, C. Cassiago, and N. De Leo, Sci. Rep. **8**, 4710 (2018).
[13] D. M. Eagles, Phys. Rev. **186**, 456 (1969).
[14] A. J. Leggett, in *Modern Trends in the Theory of Condensed Matter*, edited by A. Pekelski and J. Przystawa (Springer-Verlag, Berlin, 1980), p. 13.
[15] Q. Chen, J. Stajic, S. Tan, and K. Levin, Phys. Rep. **412**, 1 (2005).
[16] G. C. Strinati, P. Pieri, G. Röpke, P. Schuck, and M. Urban, Phys. Rep. **738**, 1 (2018).
[17] A. A. Shanenko, M. D. Croitoru, A. Vagov, and F. M. Peeters, Phys. Rev. B **82**, 104524 (2010).
[18] Y. Chen, A. A. Shanenko, A. Perali, and F. M. Peeters, J. Phys.: Condens. Matter **24**, 185701 (2012).
[19] D. Innocenti, N. Poccia, A. Ricci, A. Valletta, S. Caprara, A. Perali, and A. Bianconi, Phys. Rev. B **82**, 184528 (2010).
[20] M. V. Mazziotti, A. Valletta, G. Campi, D. Innocenti, A. Perali, and A. Bianconi, Eur. Phys. Lett. **118**, 37003 (2017).
[21] A. Guidini and A. Perali, Supercond. Sci. Technol. **27**, 124002 (2014).
[22] S. Borisenko, Nat. Mater. **12**, 600 (2013).
[23] Y. Lubashevsky, E. Lahoud, K. Chashka, D. Podolsky, and A. Kanigel, Nat. Phys. **8**, 309 (2012).
[24] S. Kasahara, T. Watashige, T. Hanaguri, Y. Kohsaka, T. Yamashita, Y. Shimoyama, Y. Mizukami, R. Endo, H. Ikeda, K. Aoyama, T. Terashima, S. Uji, T. Wolf, H. von Löhneysenn, T. Shibauchi, and Y. Matsuda, Proc. Natl. Acad. Sci. (USA) **111**, 16309 (2014).
[25] H. Miao, T. Qian, X. Shi, P. Richard, T. K. Kim, M. Hoesch, L. Y. Xing, X.-C. Wang, C.-Q. Jin, J.-P. Hu, and H. Ding, Nat. Commun. **6**, 6056 (2015).
[26] C. A. R. Sá de Melo, M. Randeria, and J. R. Engelbrecht, Phys. Rev. Lett. **71**, 3202 (1993).
[27] A. Perali, P. Pieri, G. C. Strinati, and C. Castellani, Phys. Rev. B **66**, 024510 (2002).
[28] A. Perali, C. Castellani, C. Di Castro, M. Grilli, E. Piegari, and A. A. Varlamov, Phys. Rev. B **62**, R9295(R) (2000).

[29] S. Wolf, A. Vagov, A. A. Shanenko, V. M. Axt, A. Perali, and J. A. Aguiar, Phys. Rev. B **95**, 094521 (2017).
[30] H. Suhl, B. T. Matthias, and L. R. Walker, Phys. Rev. Lett. **3**, 552 (1959).
[31] V. A. Moskalenko, Phys. Met. Metallogr. **8**, 25 (1959).
[32] B. T. Geilikman, R. O. Zaitsev, and V. Z. Kresin, Sov. Phys. Solid State **9**, 642 (1967).
[33] V. Z. Kresin, J. Low Temp. Phys. **11**, 519 (1973).
[34] I. N. Askerzade, A. Gencer, and N. Güclü, Supercond. Sci. Technol. **15**, L13 (2002).
[35] M. E. Zhitomirsky and V.-H. Dao, Phys. Rev. B **69**, 054508 (2004).
[36] V. G. Kogan and J. Schmalian, Phys. Rev. B **83**, 054515 (2011).
[37] A. A. Shanenko, M. V. Milošević, F. M. Peeters, and A. V. Vagov, Phys. Rev. Lett. **106**, 047005 (2011).
[38] A. Vagov, A. A. Shanenko, M. V. Milošević, V. M. Axt, and F. M. Peeters, Phys. Rev. B **86**, 144514 (2012).
[39] N. V. Orlova, A. A. Shanenko, M. V. Milošević, F. M. Peeters, A. V. Vagov, and V. M. Axt, Phys. Rev. B **87**, 134510 (2013).
[40] A. Larkin and A. Varlamov, *Theory of Fluctuations in Superconductors* (Oxford University Press, Oxford, 2005).
[41] S.-k. Ma, *Modern Theory of Critical Phenomena* (Westview, New York, 1976).
[42] V. N. Popov, *Functional Integrals in Quantum Field Theory and Statistical Physics* (Springer, The Netherlands, 1983).
[43] A. Griffin, T. Nikuni, and E. Zaremba, *Bose-Condensed Gases at Finite Temperatures* (Cambridge University Press, Cambridge, 2009).
[44] D. R. Nelson and J. M. Kosterlitz, Phys. Rev. Lett. **39**, 1201 (1977).
[45] A. Vagov, A. A. Shanenko, M. V. Milosevic, V. M. Axt, V. M. Vinokur, J. A. Aguiar, and F. M. Peeters, Phys. Rev. B **93**, 174503 (2016).
[46] J. B. Ketterson and S. N. Song, *Superconductivity* (Cambridge University Press, Cambridge, 1999).
[47] E. Langmann, C. Triola, and A. V. Balatsky, Phys. Rev. Lett. **122**, 157001 (2019).
[48] A. Bianconi and T. Jarlborg, Eur. Phys. Lett. **112**, 37001 (2015).
[49] T. Hanaguri, S. Kasahara, J. Böker, I. Eremin, T. Shibauchi, and Y. Matsuda, Phys. Rev. Lett. **122**, 077001 (2019).
[50] M. Iskin and C. A. R. Sá de Melo, Phys. Rev. B **74**, 144517 (2006).
[51] S. N. Klimin, J. Tempere, G. Lombardi, and J. T. Devreese, Eur. Phys. J. B **88**, 122 (2015).
[52] G. Pagano, M. Mancini, G. Cappellini, L. Livi, C. Sias, J. Catani, M. Inguscio, and L. Fallani, Phys. Rev. Lett. **115**, 265301 (2015).
[53] A. Perali, D. Neilson, and A. R. Hamilton, Phys. Rev. Lett. **110**, 146803 (2013).
[54] S. Conti, A. Perali, F. M. Peeters, and D. Neilson, Phys. Rev. Lett. **119**, 257002 (2017).
[55] (http://www.multisuper.org)
[56] J. M. Kosterlitz and D. J. Thouless, J. Phys. C **6**, 1181 (1973).